AN ANALYSIS OF CREEP CRACK GROWTH OF INTERFACE CRACKS IN LAYERED/GRADED MATERIALS

S. B. BINER
Ames Laboratory, Iowa State University
Ames, IA 50011

ABSTRACT:

In this study, the growth behavior of interface cracks in bimaterials and in layered materials resulting from the creep cavitation was studied. The growth model includes the effects of material deposition resulting from the growth of creep cavities on the crack tip stress fields. The results indicate that in layered materials under identical applied loading, the location of the interface crack strongly influence the amplitude of the stress field (C^*) at steady-state. Due to large variation in the distribution of the stresses ahead of the interface cracks at creep regime, depending upon the crack location, the creep crack growth rates will be significantly different from each other under identical loading for a given layered material.

INTRODUCTION :

The layered/graded materials hold great promise for high temperature structural applications because they permit components to be designed with tailored properties which reduce both the processing and operationally induced residual stresses to acceptable minimum levels[1]. In recent years substantial progress has been made on the mechanics of interface fracture; excellent summaries can be found in ref.[2,3]. These analyses are mostly confined to the assessment of fracture behavior at room temperature; the behavior of interface cracks at creep regime and the role of material parameters on the evolution of time dependent stress-strain fields have not been explored in detail. However, a good understanding of the mechanics of interface cracks for both temperature ranges could be most valuable in the design of these structural components through intelligent manipulation of the interfacial behavior.

The stress and strain rate response of a homogeneous isotropic material undergoing creep deformation is generally modeled using a power-law constitutive equation:

$$\dot{\varepsilon} = \dot{\varepsilon}_o \left(\frac{\sigma}{\sigma_o} \right)^n \tag{1}$$

where, $\dot{\varepsilon}$ and σ are the von Mises equivalent strain rate and stress respectively, σ_o is the reference stress, $\dot{\varepsilon}_o$ a temperature dependent reference strain rate and n is the creep exponent. In homogenous isotropic materials, the initial response of a cracked body upon application of a load at creep regime, and for some time thereafter, is essentially elastic and the elastic stress intensity factor, K, provides an adequate description of the crack tip stress-strain field. Once a steady state has been achieved, the stress-strain fields near the crack tip have a *HRR* singularity with the amplitude given by a path independent integral C^*, the rate dependent *J*-integral[4,5], i.e.:

MASTER

DISCLAIMER

**Portions of this document may be illegible
in electronic image products. Images are
produced from the best available original
document.**

$$\sigma_{ij} = \left[\frac{C^*}{\varepsilon_o I_n r}\right]^{\frac{1}{n+1}} \sigma_{ij}(\theta, n) \tag{2}$$

In eq.3 the angular dependency of the stress field σ_{ij} and integration constant I_n also depend on the creep exponent n.

It has been shown[6-8] that, in the elastic regime, the near-tip stress field for an interface crack between two dissimilar isotropic materials is a linear combination of two types of singularities, namely a coupled oscillatory field scaled by a complex K and a non-oscillatory field scaled by a usual K_{III}:

$$\sigma_{ij} = \frac{Re(K r^{i\eta})}{\sqrt{2\pi r}}\sigma_{ij}'(\theta, \eta) + \frac{Im(K r^{i\eta})}{\sqrt{2\pi r}}\sigma_{ij}''(\theta, \eta) + \frac{K_{III}}{\sqrt{2\pi r}}\sigma_{ij}'''(\theta) \tag{3}$$

where, η is bimaterial constant and the dimensionless angular functions $\sigma_{ij}'(\theta, \eta)$ and $\sigma_{ij}''(\theta, \eta)$ are also given in ref.[8]. When $\eta=0$, $\sigma_{ij}'(\theta, \eta)$ and $\sigma_{ij}''(\theta, \eta)$ reduce to the standard mode-I and mode-II angular functions.

In a previous study, the evolution of the time-dependent stress fields ahead of the stationary interface cracks in bimaterials and in layered materials at creep regime was elucidated using a finite element method[9,10]. In this study, the observed stress states for that interface cracks are incorporated into a creep crack growth model to study the evolution of the creep crack growth rates resulting from the growth of the cavities ahead of the interface cracks.

TIME DEPENDENT STRESS FIELDS AHEAD OF THE INTERFACE CRACKS :

The cases investigated in this study are schematically summarized in Fig.1. The stress-strain response of the creeping sector and the transitional layer at creep regime was assumed to obey the power law constitutive relationship (eq.1). The ε_o in eq.1 provides a natural time scale (i.e., $1/\dot{\varepsilon}$). In this study, all rate dependent variables and also the rate dependent results were scaled with the reference strain rate of the creeping sectors, $\dot{\varepsilon}_o^c$. For the creeping sector, the value of creep exponent was taken as $n=3$. Furthermore, Young's modulus relating the elastic strain increments was taken as $E=10^3\sigma_o$ and Poisson's ratio was chosen as $v=0.3$. The Young's modulus of the elastic sector was taken as three times that of the creeping sector. The layered region is assumed to be a transition region between these two extreme regions. Therefore a composite behavior was assumed for this transition layer with a Young's modulus of 1.5 times of that the creeping sector. The creep properties of this transitional layer were chosen as $n=5$ and $\dot{\varepsilon}_o' = 10^{-4}\dot{\varepsilon}_o^c$. Furthermore, the properties of this layer was also assumed to be constant from one interface to the another. For the crack configurations shown in Fig.1, the resulting C^* values and distribution of the stress components with the radial distance ahead of the cracks are summarized in Table-I and Fig.3 respectively. The other details can be found in refs.[9,10].

CREEP CAVITATION AND GROWTH OF INTERFACE CRACKS:

To simulate the growth of interface cracks resulting from the growth of the cavities, the constitutive model developed in refs.[11,12] was adopted. For cavities located ahead of an interface crack as shown schematically in Fig .2, if the cavity radius is a, and the average spacing is $2b$ the volumetric growth rate is expressed as:

$$\dot{V} = \dot{V}_1 + \dot{V}_2 \tag{4}$$

where $\dot{V}_1$ is the contribution to the volumetric growth rate due to grain boundary diffusion and given by:

$$\dot{V}_1 = 4\pi D \frac{\sigma_n - (1-f)\sigma_s}{\ln(1-f) - (3-f)(1-f)/2} \tag{5}$$

where

$$f = \max\left[\frac{a^2}{b^2}, \frac{a^2}{(a+1.5L)^2}\right] \tag{6}$$

and D is the grain boundary diffusion parameter, σ_n is the average stress normal to the current orientation of the grain boundary in the vicinity of the cavity, σ_s is the sintering stress and the parameter L serves as a stress and temperature dependent length scale governing the coupling between diffusive and creep contributions to cavity growth. $\dot{V}_2$, the contribution to the volumetric growth rate due to dislocation creep in eq.4 is expressed by:

$$\dot{V}_2 = \begin{cases} 2\pi\dot{\varepsilon}\, a^3 h(\psi)[\alpha_n + \beta_n]^n & if \left|\dfrac{\sigma_m}{\sigma_e}\right| \le 1 \\[3mm] Sign(\sigma_m)2\pi\dot{\varepsilon}\, a^3 h(\psi)\left[\alpha_n\left|\dfrac{\sigma_m}{\sigma_e}\right| + \beta_n\right]^n & if \left|\dfrac{\sigma_m}{\sigma_e}\right| > 1 \end{cases} \tag{7}$$

where

$$\alpha_n = 3/2n, \qquad \beta_n = (n-1)(n+0.4319)/n^2$$
$$h(\psi) = [(1+\cos\psi)^{-1} - 0.5\cos\psi]/\sin\psi \tag{8}$$

in which σ_m and σ_e are the average mean and effective stress respectively. The ψ is the cavity tip angle as shown in Fig.2. With these definitions, the parameter L in eq.6 is described as:

$$L = (D\sigma_e / \dot{\varepsilon})^{1/3} \tag{9}$$

L serves as a stress and temperature dependent length scale. For $a/L \le 0.1$ cavity growth is completely dominated by diffusion, whereas, for higher values of a/L creep deformation plays an increasing role[12]. With V according to eq.4 the rate of change in the cavity radius is then:

$$\dot{a} = \frac{\dot{V}}{4\pi a^2 h(\psi)} \tag{10}$$

As the cavities ahead of the crack grow, the material is deposited on the adjacent grain boundaries. This leads to a local relaxation in the normal stress acting on the cavities. The effect of material deposition on the stress field ahead of a crack was modeled by a series of edge dislocations

for each cavity as described in [13-15]. This is summed over all N cavities, then added to the normal stress, $\sigma_{\theta\theta}$, caused by remote loading to obtain the net stress on the individual cavities;

$$\sigma_n(k) = \sigma_{\theta\theta} + \frac{\mu}{4\pi b(1-\nu)} \sum_{j=1}^{N} \frac{\delta_{j+1} - \delta_j}{(k-j-1/2)} \sqrt{\frac{j}{k-1/2}} \qquad (11)$$

For interface cracks the effective shear modulus μ^* is described by[16]:

$$\frac{2}{\mu^*} = \frac{1}{\mu_1} + \frac{1}{\mu_2} \qquad (12)$$

In the simulations, the crack growth rates were obtained by integrating the eqs.4-10 using an Euler integration scheme. The initial stress values and crack tip parameters required during the solution were provided from the FEM analyses as given earlier in Fig.3 and also using eqs.2 and3 with appropriate values given in Table-1. After each time increment, the normal stress component was modified according to eq.11 and the sintering stress σ_s in eq.5 was omitted during the solution. For all cases, the growing number of cavities ahead of the crack tip was taken as $N=50$, and this value was also kept constant during the crack growth. The coalescence of the first cavity ahead of the crack tip with the crack is assumed to occurs when $a/b \geq 0.6$. Then a new cavity was nucleated at a distance of $2(N-1/2)b$ from the current tip. The half cavity spacing b was chosen as $b/W = 4\times10^{-4}$, W being the length of the original uncracked ligament, and the initial cavity radius a was taken as $a/b = 0.02$. For the K controlled crack growth cases, the increments in the K values due to crack advance in homogeneous cases were calculated from the solution available for SEN geometry[17]. Similarly, for the C^* controlled crack growth cases, the increments in the C^* values were calculated by using the appropriate creep parameters in the solutions provided in ref.[18].

The growth of the interface cracks resulting from the growth of cavities under the K controlled stress field was studied first. For these cases the a/l ratio appearing in the constitutive relation was chosen as 0.0125 which gives a mostly diffusion dominated cavity growth. The correlation of the observed creep crack growth rates with stress intensity factor for these cases are shown in Fig.4. In this figure the stress intensity factors for the interface cracks correspond to the complex stress intensity factor and for homogenous cases the stress intensity factors correspond to the usual one. For interface cracks neighboring with the creeping sector (Fig.1a and b), the crack growth rates are about twice as high as seen for a crack in the creeping sector as homogenous isotropic case. Similarly, for interface cracks located between the transitional layer and the elastic sector (Figs.1c) the growth rate is almost an order of magnitude faster than the one seen for a homogenous crack in the transitional layer.

In the following simulations, the creep crack growth rates of the interface cracks under C^* controlled regime were studied. For these cases, the steady-state stress distributions shown in Fig.3 and the initial C^* values given in Table.1 are used. In these simulations, the a/l ratio appearing in the constitutive model was taken as 0.125, yielding a more significant contribution of the creep deformation to the cavity growth. For these cases, the correlation of the crack growth rates with C^* are shown in Fig.5. As can be seen from the figure, the crack growth rates between the cases were significantly different owing to the aforementioned evolution of the largely different stress-states ahead of the interface cracks (Fig.3).

Even tough the applied loads and initial crack lengths were identical, significantly different creep growth rates were of the interface cracks are seen in Figs.4 and 5. For both K and C^* controlled growth, much faster growth rates of the interface cracks than the growth rate of a

homogeneous crack in the fastest creeping sector of that interface crack was observed. The difference ranged from about a factor of two, to several orders of magnitude. The present results clearly demonstrate that even tough the applied loads and the initial crack lengths are the same, dependent upon the location of the interface crack, the creep growth behavior will be significantly different from each other for a given layered/graded material.

CONCLUSIONS:
    In this study, the behavior of interface cracks in bimaterial and layered materials at creep regime in plane-strain condition and mode-I load state was studied. The results indicate that:
    1.   The growth rates of the interface cracks are much faster than the growth rate of a homogenous crack in the fastest creeping sector of that interface crack.
    2.   Due to large variation in the distribution of the stresses ahead of the interface crack tip depending upon the location, the creep rates of such cracks will be significantly different from each other at creep regime under identical applied loading for a given layered/graded material.

REFERENCES:
1. Int. Conference on "Mechanics and Physics of Layered and Graded Materials", Dovas, Switzerland, 1995. Eds. S. Suresh and A. Needleman (To be published).
2. Metal-Ceramic Interfaces; Acta-Scr. Metall. Proc. Series 4, Eds. M. Ruhle, A.G. Evans, M. F. Ashby and J.P. Hirth, Pergamon Press, New York 1990.
3. J.W. Hutchinson and Z. Suo; Advances in App. Mech. 29, 63, 1991
4. H. Riedel and J.R. Rice; "Tensile Cracks in Creeping Solids" in "Fracture Mechanics" Ed. P.C. Paris, ASTM, STP700, Philadelphia, 1979.
5. S.B. Biner., D.S. Wilkinson and D.Watt, Eng. Fract. Mech. 21, 479, 1981
6. F. Erdogan, J. App. Mech. 32, 403, 1965.
7. J.R. Rice and G.C. Shih, J. App. Mech. 32, 418, 1965.
8. J.R. Rice, Z. Suo and J.S. Wang; "Mechanics and Thermodynamics of Brittle Interfacial Failure In Bimaterial Systems" in "Meta-Ceramic Interfaces" Act-Scr. Metall. Proc. Series 4, Eds. M. Ruhle, A.G. Evans, M.F. Ashby and J.P. Hirth, Pergamon Press, New York, 269, 1990.
9 S.B. Biner , "A numerical analysis of time dependent stress fields ahead of stationary interface cracks at creep regime :Part-I interface cracks in bimaterials" Eng. Fract. Mech. (in press)
10. S.B. Biner , "A numerical analysis of time dependent stress fields ahead of stationary interface cracks at creep regime :Part-I interface cracks in layered materials" Eng. Fract. Mech. (in press)
11. V. Tvergaard, Acta Metall. 32, 1977, 1984.
12. V. Tvergaard, J. Mech. Phys. Solids, 32, 373, 1984.
13. V. Vitek, Acta Metall. Mater. 26, 1345, 1978.
15. M.D. Thouless, C.H. Hsueh and A.G. Evans, Acta Metall.31, 1675, 1983.
16. M.L. Williams, Seismol. Soc. Am. 49, 199, 1959.
17. H. Tada, P.C. Paris and G.R. Irwin, "The Stress Analysis Of Cracks Handbook" (2nd Ed.), Paris Productions Inc., St Louis, 1985.

18. V. Kumar, M.D. German and C.F. Shih, " An Engineering Approach for Elastic-Plastic Fracture Analysis" , EPRI Report NP-1931, Electric Power Research Inst. Palo Alto, CA, 1981.
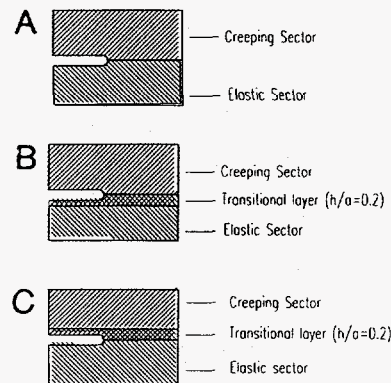
Fig.1 Schematic representation of the interface crack cases investigated in this study.
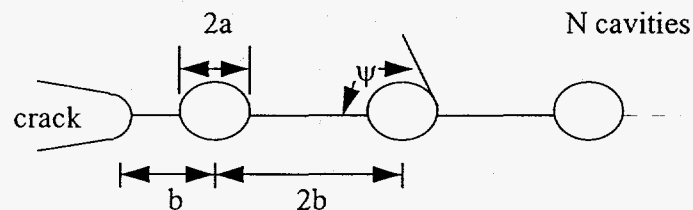

Fig.2 Schematic representation of the initial creep cavitation and the definitions of some of the parameters used in the creep crack growth model.

	$K / \sigma_o / \sqrt{W}$	$K^* / \sigma_o / \sqrt{W}$	$C^* / \sigma_o / W / \varepsilon_o^c$
Homogeneous crack in Creeping Sectors	3.57	-	31.60
Homogeneous crack in Transitional Layer	3.57	-	0.0112
Interface Crack (Fig.1a)	-	3.24	15.60
Interface Crack (Fig.1b)	-	3.36	15.20
Interface Crack (Fig.1c)	-	3.87	3.06

Table.I Summary of the initial stress intensity factors, C* values at steady-state under identical applied loading. In the table, K^* values represent the complex stress intensity factors for the interface cracks and W is the length of the uncracked ligament.
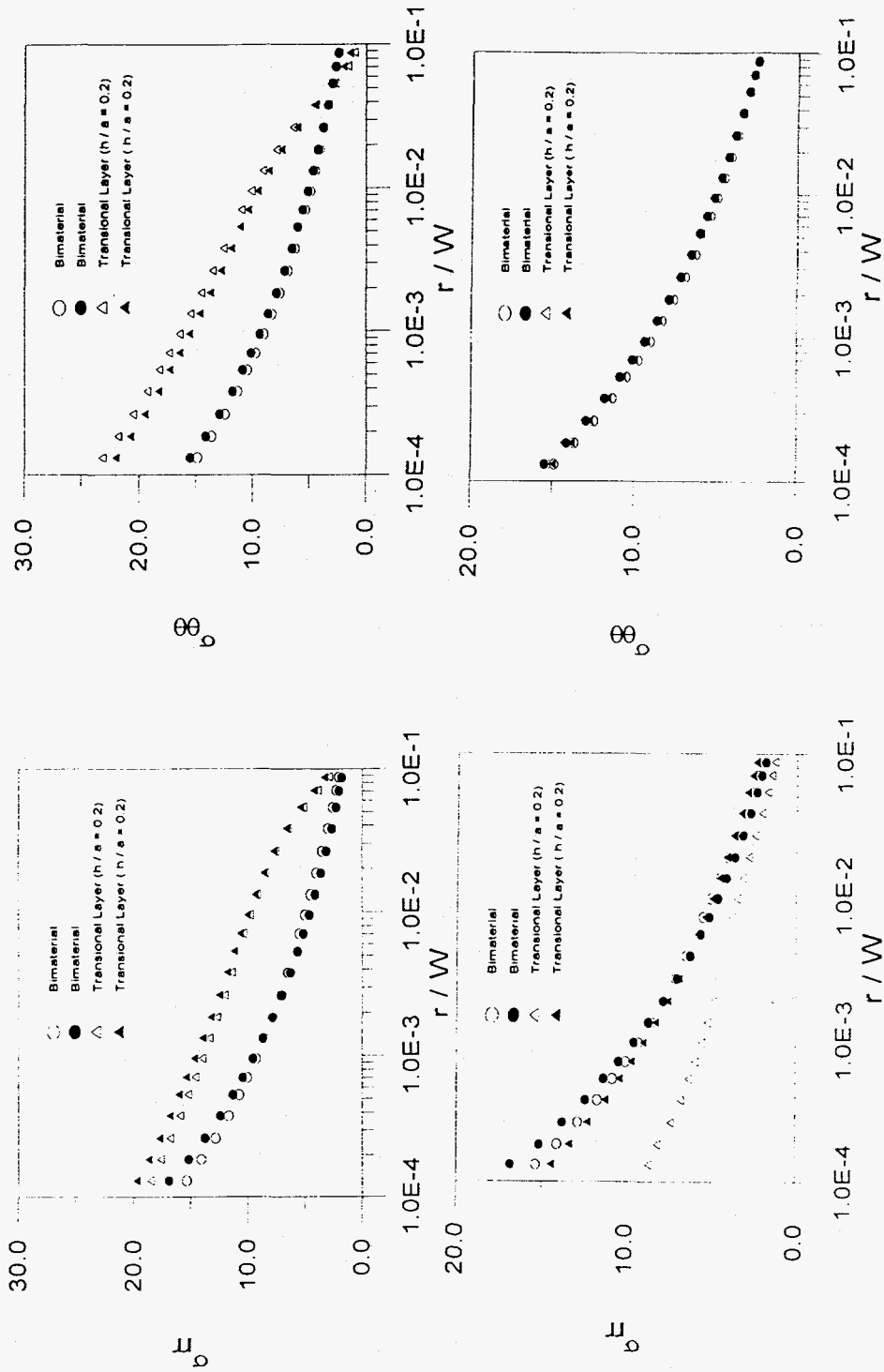
Fig.3 Comparison of the distribution of the stress components at steady-state with radial distance ahead of the interface cracks. In top figures, the interface crack is located at the interface of the elastic sector and the transitional layer, in bottom interface crack is located between the creeping sector and the transitional layer.
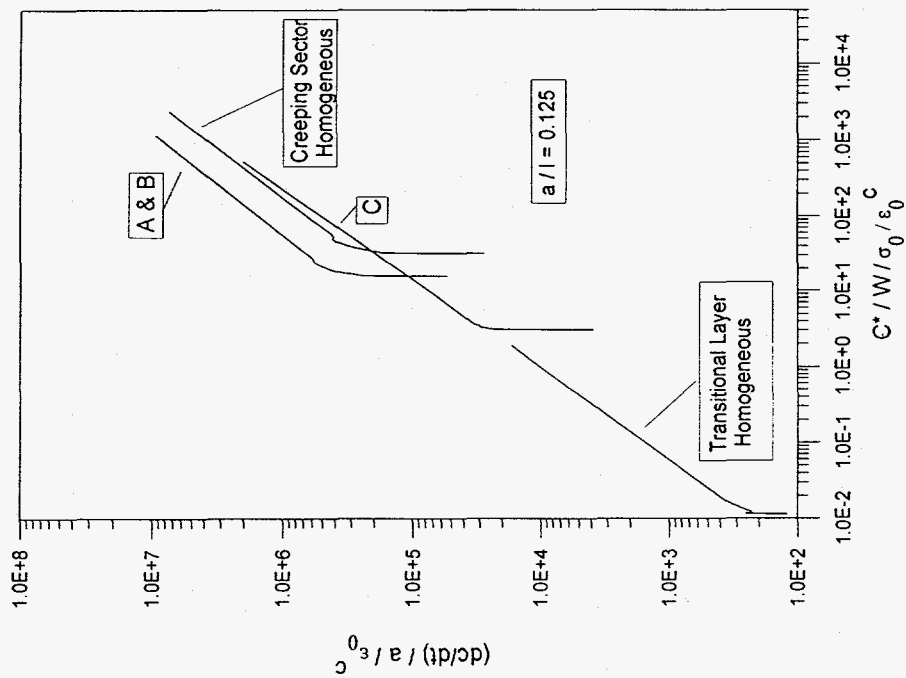
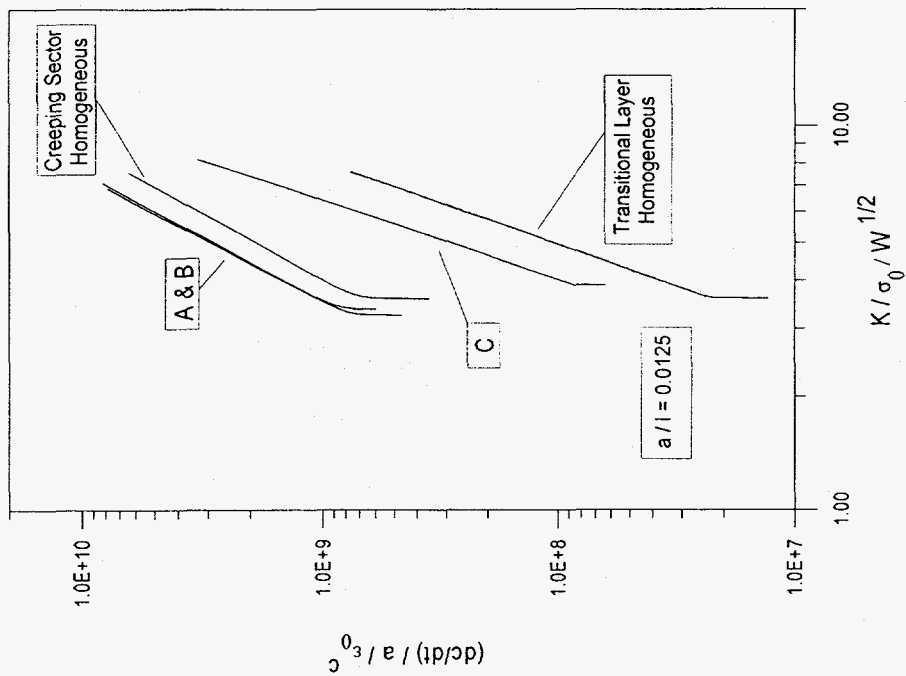Fig.5 Comparison of the growth rate of interface cracks under C* controlled stress field.

Creeping Sector Homogeneous

A & B

C

a / l = 0.125

Transitional Layer Homogeneous

$C^* / W / \sigma_0 / \varepsilon_0^c$

$(dc/dt) / a / \varepsilon_0^c$

Fig.4 Comparison of the growth rate of interface cracks under K controlled stress field.

Creeping Sector Homogeneous

A & B

C

a / l = 0.0125

Transitional Layer Homogeneous

$K / \sigma_0 / W^{1/2}$

$(dc/dt) / a / \varepsilon_0^c$